



# Growth and spectroscopic characteristics of Cr<sup>3+</sup>:CsAl(MoO<sub>4</sub>)<sub>2</sub> crystal

Guojian Wang, Lizhen Zhang, Zhoubin Lin, Guofu Wang\*

State Key Laboratory of Structural Chemistry, Fujian Institute of Research on the Structure of Matter, Chinese Academy of Sciences, No 155 Yangqiao Xilu, Fuzhou, Fujian 350002, China

## ARTICLE INFO

### Article history:

Received 12 June 2009

Received in revised form

15 September 2009

Accepted 16 September 2009

Available online 23 September 2009

### PACS:

42.70.Hj

65.40.De

78.20.-e

### Keywords:

Crystal growth

Photoelectron spectroscopic

## ABSTRACT

This paper reports the growth and spectroscopic characteristics of Cr<sup>3+</sup>:CsAl(MoO<sub>4</sub>)<sub>2</sub> crystal. A Cr<sup>3+</sup>:CsAl(MoO<sub>4</sub>)<sub>2</sub> crystal with dimensions of 42 mm × 37 mm × 10 mm has been successfully grown from a flux of Cs<sub>2</sub>Mo<sub>3</sub>O<sub>10</sub> by the TSSG method. The absorption and emission spectra were investigated. The absorption cross sections  $\sigma_a$  are  $5.05 \times 10^{-20} \text{ cm}^{-2}$  at 481 nm for the <sup>4</sup>A<sub>2</sub> → <sup>4</sup>T<sub>1</sub> transition and  $3.06 \times 10^{-20} \text{ cm}^{-2}$  at 670 nm for the <sup>4</sup>A<sub>2</sub> → <sup>4</sup>T<sub>2</sub> transition of Cr<sup>3+</sup> ions, respectively. The emission cross section  $\sigma_e$  of <sup>4</sup>T<sub>2</sub> → <sup>4</sup>A<sub>2</sub> transition is  $4.27 \times 10^{-20} \text{ cm}^2$  at 818 nm and fluorescence lifetime is 21 μs. Based on the absorption and emission spectra, the crystal field strength Dq, the Racah parameters B and C, the effective phonon energy  $\hbar\omega$  and the Huang–Rys factor S were calculated. The investigated results show that Cr<sup>3+</sup>:CsAl(MoO<sub>4</sub>)<sub>2</sub> crystal may be regarded as a potential tunable laser crystal material.

© 2009 Elsevier B.V. All rights reserved.

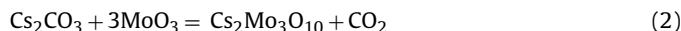
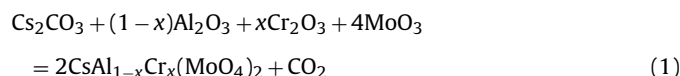
## 1. Introduction

Since tunable solid-state lasers have a wide field application in medicine, ultra short pulse generation, environment and communication, research on Cr<sup>3+</sup>-doped tunable solid-state laser in the visible and near infrared spectrum has gained strong interest [1–5]. Recently double metals molybdate and tungstate with a general formula M<sup>I</sup>M<sup>III</sup>(M<sup>VI</sup>O<sub>4</sub>)<sub>2</sub> (where M<sup>I</sup> = Na, K, Rb, Cs, M<sup>III</sup> = Al, In, Sc and M<sup>VI</sup> = Mo, W) are gaining attentions because their interesting chemical and physical properties. The Cr<sup>3+</sup>-doped M<sup>I</sup>M<sup>III</sup>(M<sup>VI</sup>O<sub>4</sub>)<sub>2</sub> materials have currently receiving a great deal of attention due to their interesting properties in tunable laser applications [6–16]. CsAl(MoO<sub>4</sub>)<sub>2</sub> is a member of this family of materials with P $\bar{3}m1$  space group and cell parameters  $a = 5.551(1) \text{ \AA}$ ,  $c = 8.037(2) \text{ \AA}$  [17]. It was reported that single crystals of Cr<sup>3+</sup>-doped CsAl(MoO<sub>4</sub>)<sub>2</sub> were grown using the Klevtsov method [18] by Hermanowicz [6]. However, the crystals with large size and high quality were difficulty obtained by this method. In this paper, we report the growth of Cr<sup>3+</sup>:CsAl(MoO<sub>4</sub>)<sub>2</sub> crystal by TSSG technique and its spectroscopic characterization.

## 2. Crystal growth

Since CsAl(MoO<sub>4</sub>)<sub>2</sub> crystal melts incongruently at 715 °C [19], Cr<sup>3+</sup>-doped CsAl(MoO<sub>4</sub>)<sub>2</sub> crystals were only grown by the top seed solution growth (TSSG) method. Cr<sup>3+</sup>-doped CsAl(MoO<sub>4</sub>)<sub>2</sub> crystals were grown from a flux of Cs<sub>2</sub>Mo<sub>3</sub>O<sub>10</sub> by the TSSG method. In order to select the suitable composition of solution, the solubility curve of CsAl(MoO<sub>4</sub>)<sub>2</sub> in CsAl(MoO<sub>4</sub>)<sub>2</sub>–Cs<sub>2</sub>Mo<sub>3</sub>O<sub>10</sub> solution was determined by means of trial seeding. The saturation temperatures were determined for various compositions in a range of 60–80 mol% Cs<sub>2</sub>Mo<sub>3</sub>O<sub>10</sub> by adjusting the temperature of the solution until a trial seeding showed no change in weight or surface micro-topography after 4–5 h immersion. Fig. 1 shows the solubility curve of CsAl(MoO<sub>4</sub>)<sub>2</sub> in the solution.

The crystal growth was carried out in a vertical tubular muffle furnace with a nickel-chrome wire as the heating element. An AL-708 controller controlled the furnace temperature and the rate of cooling. The crystal was grown in a platinum crucible with dimensions of  $\varnothing 60 \text{ mm} \times 50 \text{ mm}$ . The starting materials with 66.7 mol% Cs<sub>2</sub>Mo<sub>3</sub>O<sub>10</sub> and 33.3 mol% CsAl(MoO<sub>4</sub>)<sub>2</sub> were weighed according to following chemical reaction equations:



\* Corresponding author. Tel.: +86 591 83714636; fax: +86 591 83714636.

E-mail address: [wgf@ms.fjirsm.ac.cn](mailto:wgf@ms.fjirsm.ac.cn) (G. Wang).

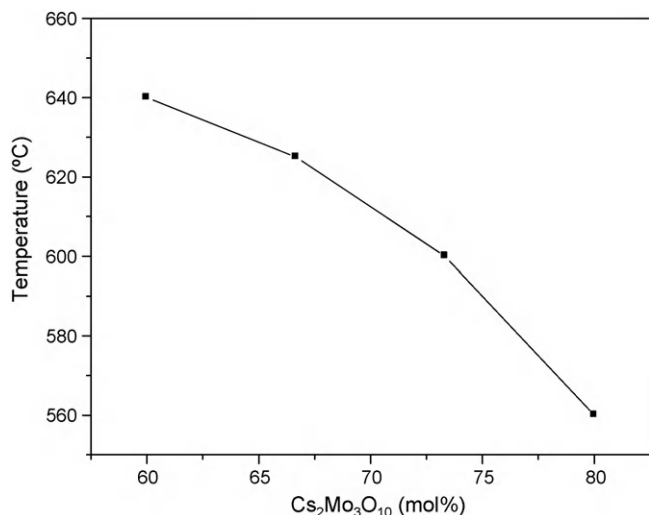


Fig. 1. Solubility curve of CsAl(MoO<sub>4</sub>)<sub>2</sub> in CsAl(MoO<sub>4</sub>)<sub>2</sub>–Cs<sub>2</sub>Mo<sub>3</sub>O<sub>10</sub> solution.

The chemicals used were Cs<sub>2</sub>CO<sub>3</sub>, Al<sub>2</sub>O<sub>3</sub> and MoO<sub>3</sub> with 99.95% purity and Cr<sub>2</sub>O<sub>3</sub> with 99.99% purity. The weighed materials with 1 at.% Cr<sub>2</sub>O<sub>3</sub> were mixed and put into the platinum crucible. The mixture of starting materials was kept at temperature 30 °C above the saturation temperature for 2 days to make the solution melt completely and homogeneously. The saturation temperature of the solution was exactly determined by repeated seeding. The crystal was grown at a cooling rate of 1–2 °C/day and rotated at a rate of 4.5 rpm. When the growth process was ended, the crystal was drawn out of the solution surface and cooled down to room temperature. Cr<sup>3+</sup>:CsAl(MoO<sub>4</sub>)<sub>2</sub> crystal with dimensions of 42 mm × 37 mm × 10 mm was obtained, as shown in Fig. 2. During the cooling process Cr<sup>3+</sup>:CsAl(MoO<sub>4</sub>)<sub>2</sub> crystals strongly tended towards cracking and cleaving. In CsAl(MoO<sub>4</sub>)<sub>2</sub> crystals, MoO<sub>4</sub> tetrahedra and AlO<sub>6</sub> octahedra built up a [AlMo<sub>2</sub>O<sub>8</sub><sup>-1</sup>] layer, the [AlMo<sub>2</sub>O<sub>8</sub><sup>-1</sup>] layers are perpendicular to the trigonal *c*-axis [17,20]. Since this layer structure of CsAl(MoO<sub>4</sub>)<sub>2</sub> crystals easily results in cleave along the [AlMo<sub>2</sub>O<sub>8</sub><sup>-1</sup>] layer, the grown CsAl(MoO<sub>4</sub>)<sub>2</sub> crystals tended towards cleaving during the cooling process under thermal stress. The cleavage plane of Cr<sup>3+</sup>:CsAl(MoO<sub>4</sub>)<sub>2</sub> crystal was determined to belong to (001) face using an YX-200 X-ray diffraction orientating instrument. The appeared faces of the grown crystal of Cr<sup>3+</sup>:CsAl(MoO<sub>4</sub>)<sub>2</sub> crystal were determined by the



Fig. 2. Photograph of the grown Cr<sup>3+</sup>:CsAl(MoO<sub>4</sub>)<sub>2</sub> crystal.

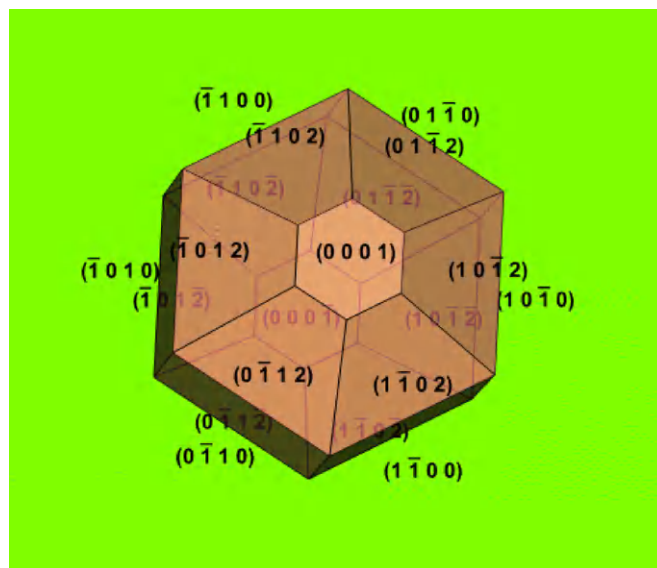


Fig. 3. Growth morphology of Cr<sup>3+</sup>:CsAl(MoO<sub>4</sub>)<sub>2</sub> crystals.

YX-200 X-ray diffraction orientating instrument, which belong to (001), (102) and ( $\bar{1}$ 10), respectively. Based on the structure of CsAl(MoO<sub>4</sub>)<sub>2</sub>, the morphological scheme of CsAl(MoO<sub>4</sub>)<sub>2</sub> crystal is drawn by WinXMorph program [21], as shown in Fig. 3.

The Cr<sup>3+</sup> ions concentration in Cr<sup>3+</sup>:CsAl(MoO<sub>4</sub>)<sub>2</sub> crystal was determined to be 2.0 at.% by ionic coupled plasma (ICP) spectrometry. The distribution coefficient is defined as following formula:

$$\eta = \frac{\text{Cr}^{3+} \text{ concentration in the crystal}}{\text{Cr}^{3+} \text{ concentration in the initial charge}} \quad (3)$$

Thus, the distribution coefficient of Cr<sup>3+</sup> ion in Cr<sup>3+</sup>:CsAl(MoO<sub>4</sub>)<sub>2</sub> crystals is 2.0.

The specific heat was measured using a NETZSCH STA 449C simultaneous thermal analyzer. Fig. 4 shows the dependence of the specific heats of Cr<sup>3+</sup>:CsAl(MoO<sub>4</sub>)<sub>2</sub> crystals on the temperature. The specific heat is 0.27 J/g K at 50 °C.

### 3. Spectral properties

A sample with dimensions of 5.0 mm × 5.2 mm × 1 mm was cut from the as-grown crystal and polished for the spectral measurement. The absorption spectrum at room temperature was recorded with a PerkinElmer UV–VIS–NIR Spectrometer (Lambda-900). The

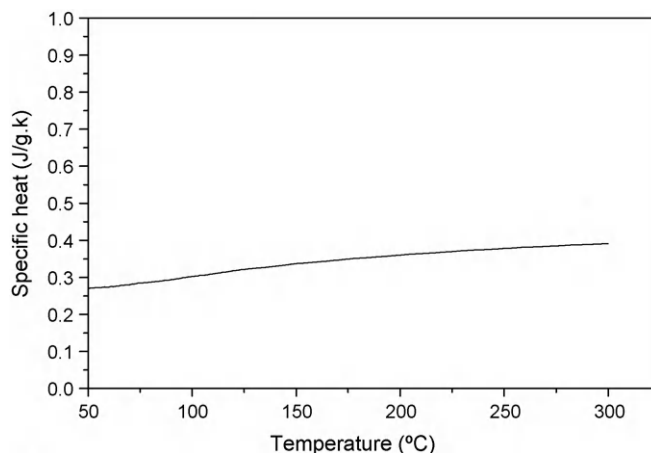


Fig. 4. Dependence of the specific heat on the temperature.

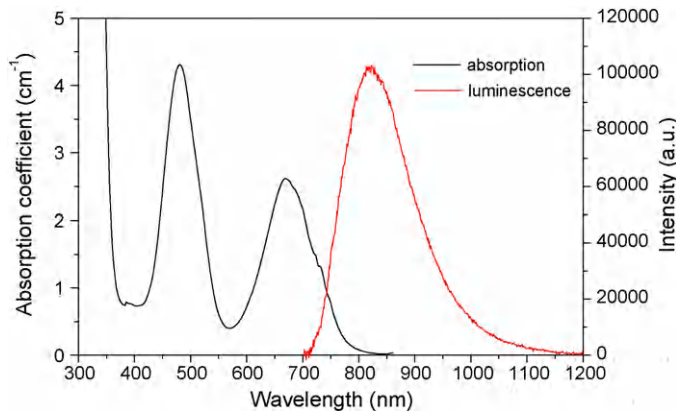


Fig. 5. Absorption and luminescence spectra of  $\text{Cr}^{3+}:\text{CsAl}(\text{MoO}_4)_2$  crystal at room temperature.

fluorescence spectrum and fluorescence lifetime were measured using an Edinburgh Instruments FLS920 spectrophotometer with a continuous Xe-flash lamp at room temperature.

Fig. 5 shows the absorption and luminescence spectra of  $\text{Cr}^{3+}:\text{CsAl}(\text{MoO}_4)_2$  crystal. The  $\text{Cr}^{3+}$  as an active ion tends to be incorporated into environments which are octahedrally coordinated by ligands. Since in the structure of  $\text{CsAl}(\text{MoO}_4)_2$  there is only one kind of  $\text{AlO}_6$  octahedron, the absorption spectrum of  $\text{Cr}^{3+}:\text{CsAl}(\text{MoO}_4)_2$  should be originated from one center of  $\text{Cr}^{3+}$  ions. The absorption spectrum consists of two broad bands, corresponding to the  ${}^4\text{A}_2 \rightarrow {}^4\text{T}_1$  transition of  $\text{Cr}^{3+}$  ion and to the  ${}^4\text{A}_2 \rightarrow {}^4\text{T}_2$  transition of  $\text{Cr}^{3+}$  ion, respectively. The absorption cross section  $\sigma_a$  were determined using  $\sigma_a = \alpha/N_c$ , where  $\alpha$  is the absorption coefficient,  $N_c$  is the concentration of  $\text{Cr}^{3+}$  ions in  $\text{Cr}^{3+}:\text{CsAl}(\text{MoO}_4)_2$ , which is  $8.56 \times 10^{19}$  ions/cm<sup>3</sup>. Then the absorption cross section  $\sigma_a$  is  $5.05 \times 10^{-20}$  cm<sup>2</sup> at 481 nm for the  ${}^4\text{A}_2 \rightarrow {}^4\text{T}_1$  transition and  $3.06 \times 10^{-20}$  cm<sup>2</sup> at 670 nm for the  ${}^4\text{A}_2 \rightarrow {}^4\text{T}_2$  transition, respectively. The peak at 738.12 nm is attributed to  ${}^4\text{A}_2 \rightarrow {}^2\text{E}$  transition of  $\text{Cr}^{3+}$  ion [6].

The energies of the electronic states of  $\text{Cr}^{3+}$  ion, which are determined by the crystal field  $Dq$  and Racah parameters  $B$  and  $C$ . According to the Tanabe and Sugano diagram [22], a strong crystal field is present when  $Dq/B > 2.3$ . In this case the  ${}^4\text{T}_2$  level is above  ${}^2\text{E}$  level, the R-line and its vibronic sideband is only observed. For example, the laser action of ruby ( $\text{Cr}^{3+}:\text{Al}_2\text{O}_3$ ) is driven by the  ${}^2\text{E} \rightarrow {}^4\text{A}_2$  R-line emission. When  $Dq/B < 2.3$ , the crystal field is weak. The  ${}^4\text{T}_2$  level is below  ${}^2\text{E}$  level, the broad emission band of  ${}^4\text{T}_2 \rightarrow {}^4\text{A}_2$  transition is only observed as observed for  $\text{Cr}:\text{LiCAF}$  and  $\text{Cr}:\text{LiSAF}$  crystals. Then the  ${}^4\text{T}_2$  level is the lower one and a broadband luminescence is observed. There are also intermediate field materials where  $Dq/B \sim 2.3$ .

The strength of the crystal field  $Dq$  and Racah parameters  $B$  and  $C$  can be obtained from the absorption. The energy separations of the  ${}^4\text{T}_1$  and  ${}^4\text{T}_2$  states from  ${}^4\text{A}_2$  ground state are very sensitive to  $Dq$ , the strength of the crystal field. The peak energy of  ${}^4\text{A}_2 \rightarrow {}^4\text{T}_2$  transition measures  $10Dq$ , i.e.  $10Dq = E_a({}^4\text{T}_2)$ . The energy at the peak of the  ${}^4\text{A}_2 \rightarrow {}^4\text{T}_2$  band depends on the both  $Dq$  and  $B$  [22,23]. If  $\Delta E$  is the difference in energy at peaks of the two bands, i.e.  $\Delta E = E_a({}^4\text{T}_1) - E_a({}^4\text{T}_2)$ , then substituting the measured values of  $\Delta E = 5865$  cm<sup>-1</sup> and  $Dq = 1492.5$  cm<sup>-1</sup> into Eq. (4), determines  $B$  to be 583.1 cm<sup>-1</sup>.

$$\frac{B}{Dq} = \frac{(\Delta E/Dq)^2 - 10(\Delta E/Dq)}{15((\Delta E/Dq) - 8)} \quad (4)$$

The  $C$  can be calculated from following formula [14]:

$$C = \frac{E({}^2\text{E}) - 7.9B + 1.8B^2/Dq}{3.05} \quad (5)$$

Table 1  
Energy levels of  $\text{Cr}^{3+}$  ion in  $\text{Cr}^{3+}:\text{CsAl}(\text{MoO}_4)_2$  crystal.

$O_h$ group show ${}^{25+1} \Gamma_i$	Level	Energy (cm <sup>-1</sup> )	Energy of relative ground state (cm <sup>-1</sup> )
${}^2\text{T}_2(\text{a}^2\text{D}, \text{b}^2\text{D}, {}^2\text{F}, {}^2\text{G}, {}^2\text{H})$	$t_2^3$	-6,437	20,219
	$t_2^2({}^3\text{T}_1)\text{e}$	1,661	28,317
	$t_2^2({}^1\text{T}_2)\text{e}$	10,243	36,899
	$t_2\text{e}^2({}^1\text{A}_1)$	35,874	62,530
	$t_2\text{e}^2({}^1\text{E})$	18,079	44,735
${}^2\text{T}_1({}^2\text{P}, {}^2\text{F}, {}^2\text{G}, {}^2\text{H})$	$t_2^3$	-12,630	14,026
	$t_2^2({}^3\text{T}_1)\text{e}$	6,099	31,960
	$t_2^2({}^1\text{T}_2)\text{e}$	1,992	28,648
	$t_2\text{e}^2({}^3\text{A}_2)$	16,573	43,229
	$t_2\text{e}^2({}^1\text{E})$	22,294	48,950
${}^2\text{E}(\text{a}^2\text{D}, \text{b}^2\text{D}, {}^2\text{G}, {}^2\text{H})$	$t_2^3$	-13,122	13,534
	$t_2^2({}^3\text{A}_1)\text{e}$	19,306	45,962
	$t_2^2({}^3\text{E}_1)\text{e}$	3,583	29,378
	$\text{e}^3$	38,192	64,848
${}^4\text{T}_1({}^4\text{P}, {}^4\text{F})$	$t_2^2({}^3\text{T}_1)\text{e}$	-5,867	20,789
	$t_2\text{e}^2({}^3\text{A}_2)$	6,075	32,731
${}^4\text{T}_2({}^4\text{F})$	$t_2^2({}^3\text{T}_1)\text{e}$	-11,731	14,925
${}^2\text{A}_1({}^2\text{G})$	$t_2^2({}^1\text{E}_1)\text{e}$	-201	26,455
${}^2\text{A}_2({}^2\text{F})$	$t_2^2({}^1\text{E}_1)\text{e}$	11,461	38,117
${}^4\text{A}_2({}^4\text{F})$	$t_2^3$	-26,656	0

Using the value  $E({}^2\text{E}) = 13,548$  cm<sup>-1</sup> and the values of  $Dq$  and  $B$ , the  $C$  was calculated to be 3066 cm<sup>-1</sup>.

The energy levels of  $\text{Cr}^{3+}:\text{CsAl}(\text{MoO}_4)_2$  crystal can be calculated when the values of  $Dq$ ,  $B$  and  $C$  are substituted in the secular equation [24]. Then the energy levels of  $\text{Cr}^{3+}:\text{CsAl}(\text{MoO}_4)_2$  crystal are listed in Tables 1 and 2 show the calculated values are in good agreement with the experimental values for  $\text{Cr}^{3+}:\text{CsAl}(\text{MoO}_4)_2$  crystal.

The luminescence spectrum of  $\text{Cr}^{3+}:\text{CsAl}(\text{MoO}_4)_2$  crystal excited with 670 nm radiation at room temperature is shown in Fig. 5. The dominant feature of luminescence of  $\text{Cr}^{3+}:\text{CsAl}(\text{MoO}_4)_2$  crystal is broad emission band with peak at 818 nm, corresponding to the  ${}^4\text{T}_2 \rightarrow {}^4\text{A}_2$  transition.  $Dq/B = 2.55 > 2.3$  of  $\text{Cr}^{3+}:\text{CsAl}(\text{MoO}_4)_2$  crystal implies that the energy level of  ${}^4\text{T}_2$  is higher than that of  ${}^2\text{E}$ , therefore, the line emission of  ${}^2\text{E} \rightarrow {}^4\text{A}_2$  transition should be visible. However, only the  ${}^4\text{T}_2 \rightarrow {}^4\text{A}_2$  transition is observed on the photoluminescence spectrum at 300 K. This could be explained by the increased thermal population of the  ${}^4\text{T}_2$  level with increasing temperature as well as by two orders of magnitude greater probability for the  ${}^4\text{T}_2 \rightarrow {}^4\text{A}_2$  transition than that for the  ${}^2\text{E} \rightarrow {}^4\text{A}_2$  transition to take place [11]. These means  $\text{Cr}^{3+}$  ions occupy intermediate crystal field sites in  $\text{Cr}^{3+}:\text{CsAl}(\text{MoO}_4)_2$  crystal.

The emission cross section  $\sigma_e$  was determined by the following formula [25]:

$$\sigma_e = \frac{\lambda^2}{4\pi^2 \tau_f n^2 \Delta\nu} \quad (6)$$

where  $n$  is refractive index which was estimated to be 1.72 by Abbe Refractometer at 589 nm wavelength.  $\lambda$  is the emission wavelength, the  $\Delta\nu$  is the half-band frequency and  $\tau_f$  is fluorescence lifetime. The luminescence lifetime of  ${}^4\text{T}_2 \rightarrow {}^4\text{A}_2$  transition was measured to be 21  $\mu\text{s}$ , as shown in Fig. 6. Then, the emission cross section  $\sigma_e$  at 818 nm is  $4.27 \times 10^{-20}$  cm<sup>2</sup>.

Table 2  
Theory and experiment values of  $\text{Cr}^{3+}:\text{CsAl}(\text{MoO}_4)_2$  crystal.

Level	Theory value (cm <sup>-1</sup> )	Experiment values (cm <sup>-1</sup> )	Relative error (%)
${}^2\text{E}(t_2^3)$	13,534	13,548	0.1
${}^4\text{T}_2(t_2^2({}^3\text{T}_1)\text{e})$	14,925	14,925	0
${}^4\text{T}_1(t_2^2({}^3\text{T}_1)\text{e})$	20,789	20,790	0.005

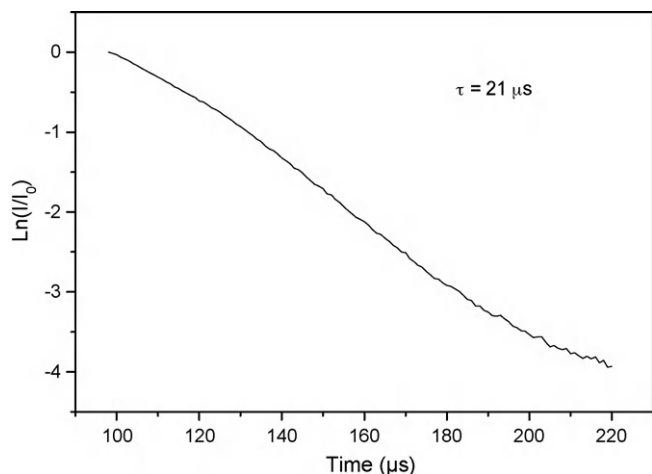


Fig. 6. Luminescence decay curve of  $\text{Cr}^{3+}:\text{CsAl}(\text{MoO}_4)_2$  crystal at room temperature.

Having luminescence spectrum, the effective phonon energy  $\hbar\omega$  and the Huang–Rhys factor  $S$  can be obtained. For oxides the effective phonon energy can be expressed in the following equation [26]:

$$\hbar\omega \approx 2.25 E_a \left[ \frac{0.3456}{E_a - E_e} \right]^{1/2} \quad (7)$$

where  $E_a$  is the peak energy absorption spectrum ( ${}^4\text{A}_2 \rightarrow {}^4\text{T}_2$  transition) and  $E_e$  is the peak energy of emission spectrum ( ${}^4\text{T}_2 \rightarrow {}^4\text{A}_2$  transition).

The Huang–Rhys factor  $S$  is related with the difference in energy between the absorption and emission band peaks (Stokes shift,  $E_s = E_a - E_e$ ) by following expression [26]:

$$E_s = 2S\hbar\omega \quad (8)$$

Thereupon,  $E_s = 2700 \text{ cm}^{-1}$ ,  $\hbar\omega = 379.9 \text{ cm}^{-1}$  and  $S = 3.55$  can be obtained by the experimental values of  $E_a = 14,925 \text{ cm}^{-1}$  and  $E_e = 12,225 \text{ cm}^{-1}$ .  $\text{Cr}^{3+}$  ions in  $\text{CsAl}(\text{MoO}_4)_2$  crystal have a stronger coupling to the crystal lattice than that in other some fluoride crystals (such as  $\text{K}_2\text{NaScF}_6$ ,  $\text{ScF}_3$ ,  $\text{K}_2\text{NaGaF}_6$ , etc.) [26].

#### 4. Conclusion

A  $\text{Cr}^{3+}:\text{CsAl}(\text{MoO}_4)_2$  crystal with dimensions of  $42 \text{ mm} \times 37 \text{ mm} \times 10 \text{ mm}$  has been grown from a flux of  $\text{Cs}_2\text{Mo}_3\text{O}_{10}$  by the TSSG method. The solubility curve of  $\text{CsAl}(\text{MoO}_4)_2$  in the  $\text{CsAl}(\text{MoO}_4)_2\text{--Cs}_2\text{Mo}_3\text{O}_{10}$  solution was measured. The distribution coefficient of  $\text{Cr}^{3+}$  ion in  $\text{Cr}^{3+}:\text{CsAl}(\text{MoO}_4)_2$  crystals is 2.0 which is over 1.0. Such large coefficient shows that the  $\text{Cr}^{3+}$  ions  $\text{CsAl}(\text{MoO}_4)_2$  crystal are easily incorporated into  $\text{CsAl}(\text{MoO}_4)_2$  crystal, but it may result in the inhomogeneous distribution of  $\text{Cr}^{3+}$  ions in  $\text{Cr}^{3+}:\text{CsAl}(\text{MoO}_4)_2$  crystal. Based on the absorption and emis-

sion spectra, the crystal field strength  $Dq$ , the Racah parameters  $B$  and  $C$ , the effective phonon energy  $\hbar\omega$  and the Huang–Rhys parameter  $S$  were calculated:  $Dq = 1492.5 \text{ cm}^{-1}$ ,  $B = 583.1 \text{ cm}^{-1}$  and  $C = 3066 \text{ cm}^{-1}$ ,  $\hbar\omega = 379.9 \text{ cm}^{-1}$  and the Huang–Rhys parameter  $S = 3.55$ . The absorption cross section  $\sigma_a$  of  ${}^4\text{A}_2 \rightarrow {}^4\text{T}_1$  and  ${}^4\text{A}_2 \rightarrow {}^4\text{T}_2$  transitions are  $5.05 \times 10^{-20} \text{ cm}^{-2}$  and  $3.06 \times 10^{-20} \text{ cm}^{-2}$ , respectively. The large absorption cross sections mean that is suitable for efficient pumping with commercial laser diodes such as  $\text{AlGaInP}$  whose emission wavelength ranges 670–690 nm. At room temperature the luminescence spectrum of  $\text{Cr}^{3+}:\text{CsAl}(\text{MoO}_4)_2$  crystal has a broad emission of wide tunable range (700–1200 nm) with FWHM of 147 nm. The emission cross section  $\sigma_e$  of  ${}^4\text{T}_2 \rightarrow {}^4\text{A}_2$  transition is  $4.27 \times 10^{-20} \text{ cm}^2$  and fluorescence lifetime is 21  $\mu\text{s}$ . In conclusion, the investigated results show that  $\text{Cr}^{3+}:\text{CsAl}(\text{MoO}_4)_2$  crystal may be regarded as a potential tunable laser crystal material.

#### Acknowledgments

This work is supported by the National Natural Science Foundation of China (No. 60978054) and the Young Scientists Innovation Foundation of Fujian Province (2008F3113), respectively.

#### References

- [1] G.J. Wang, Z.B. Lin, L.Z. Zhang, Y.S. Huang, G.F. Wang, J. Lumin. 129 (2009) 1398.
- [2] E. Cavalli, A. Belletti, M.G. Brik, J. Phys. Chem. Solids 69 (2008) 29.
- [3] D. Ivanova, V. Nikolov, R. Todorov, J. Cryst. Growth 311 (2009) 3428.
- [4] U. Demirbas, A. Sennaroglu, F.X. Kärtner, J.G. Fujimoto, J. Opt. Soc. Am. B 26 (2009) 64.
- [5] U. Demirbas, A. Sennaroglu, F.X. Kärtner, J.G. Fujimoto, Opt. Lett. 34 (2009) 497.
- [6] K. Hermanowicz, J. Lumin. 109 (2001) 9.
- [7] K. Hermanowicz, M. Maczka, M. Deren, J. Hanuza, W. Strek, H. Drulis, J. Lumin. 92 (2001) 151.
- [8] K. Hermanowicz, J. Alloys Compd. 341 (2001) 179.
- [9] W.C. Zhang, Q. Zhou, M. Yang, X.X. Wu, Opt. Mater. 27 (2004) 449.
- [10] A. Peña, R. Solé, J. Gavalda, F. Massons, F. Díaz, M. Aguiló, Chem. Mater. 18 (2006) 442.
- [11] I. Nikolov, X. Mateos, F. Güell, J. Massons, V. Nikolov, P. Peshev, F. Díaz, Opt. Mater. 25 (2004) 53.
- [12] K. Hermanowicz, J. Hanuza, M. Maczka, P.J. Dereń, E. Mugeński, H. Drulis, I. Sokolska, J. Sokolnicki, J. Phys. Condens. Matter 13 (2001) 5807.
- [13] A.J. Mao, X.Y. Kuang, H. Wang, X.F. Huang, J. Alloys Compd. 448 (2008) 6.
- [14] G.J. Wang, X.F. Long, L.Z. Zhang, G.F. Wang, J. Cryst. Growth 310 (2008) 624.
- [15] G.J. Wang, X.F. Long, L.Z. Zhang, G.F. Wang, S. Polosan, T. Tsuboi, J. Lumin. (2008) 1556.
- [16] G.J. Wang, X.M. Han, M.J. Song, Z.B. Lin, G.F. Wang, X.F. Long, Mater. Lett. 61 (2007) 3886.
- [17] P.E. Tomaszewski, A. Pieteraszko, M. Maczka, J. Hanuza, Acta Crystallogr. E58 (2002) 1119.
- [18] P.V. Klevtsov, L.P. Kozeeva, L.Y. Khartchenko, Kristallografiya 20 (1975) 1210.
- [19] V.K. Trunov, V.A. Efremov, Zh. Neorgan. Khim. 16 (1971) 2026.
- [20] P.V. Klevtsov, R.F. Klevtsova, J. Struct. Chem. 18 (1977) 339.
- [21] W. Kaminsky, J. Appl. Cryst. 40 (2007) 382.
- [22] Y. Tanabe, S. Sugano, J. Phys. Soc. Jpn. 9 (1954) 753.
- [23] B. Henderson, G.F. Imbush, Optical Spectroscopy of Inorganic Crystals, Oxford University Press, Oxford, 1989.
- [24] Y. Tanabe, S. Sugano, J. Phys. Soc. Jpn. 9 (1954) 766.
- [25] X.F. Long, Z.B. Lin, Z.S. Hu, G.F. Wang, Chem. Phys. Lett. 392 (2004) 192.
- [26] Z.D. Luo, Y.D. Huang, J. Phys. Condens. Matter 5 (1993) 9411.